THE ASTROPHYSICAL JOURNAL, 450:585–592, 1995 September 10

THE UNUSUAL QUASAR PG 1407+265

JONATHAN C. MCDOWELL,[1] CLAUDE CANIZARES,[2] MARTIN ELVIS,[1] ANDREW LAWRENCE,[3]
SERA MARKOFF[4], SMITA MATHUR,[1] AND BELINDA J. WILKES[1]
Received 1994 December 27; accepted 1995 March 24

ABSTRACT

PG 1407+265, discovered in the Palomar-Green Survey (Schmidt & Green 1983), was identified as a $z \sim 1$ radio-quiet quasar on the basis of a single weak line. Further observations over a wide wavelength range confirm the identification but reveal the object to have unusual emission-line properties. Broad Hα is the only strong emission line with Hβ and Lyman-α almost undetectably weak. The emission lines show a range in redshift of over 10,000 km s^{-1}, systematically decreasing with ionization potential or, almost equivalently, increasing to longer wavelengths. A value of $z = 0.94 \pm 0.02$ is a reasonable statement of our knowledge of the quasar's redshift. However, the object's continuum properties are those of a normal radio-quiet quasar. We discuss a number of possible models for the object, but its nature remains puzzling.

Subject heading: quasars: individual (PG 1407+265)

1. INTRODUCTION

In the course of our survey of quasar continuum energy distributions (Elvis et al. 1994), we realized that the redshift of one of our sample objects, PG 1407+265, was not secure. The assignment of $z = 0.944$ by Schmidt & Green (1983) was based on a single extremely weak line identified as Mg II λ2798. Noisy *IUE* spectra obtained in 1983 and 1987 did not reveal any further lines. Confidence in the identification was increased with the publication of a high-quality optical by Steidel & Sargent (1991) which showed weak Fe II emission in addition to the Mg II line, but a 1989 *IUE* spectrum of improved quality by P. O'Brien failed to show any evidence for hydrogen Lyman-α.

We have carried out a comprehensive multiwaveband study (Table 1) of this object as part of our larger survey of quasar properties (Elvis et al. 1994). Our optical spectrophotometry showed no evidence for significant variability over a baseline of 10 yr; this, the lack of polarization (Berriman et al. 1990), and the radio-quiet nature of the source make it unlikely that it is related to BL Lac objects. The X-ray flux detected by the *Einstein* and *ROSAT* satellites is at the level expected for a quasar, and the continuum shape is normal with an ultraviolet bump of median strength and, as expected, an inflection at between 1 and 2 μm in the putative rest frame. Nevertheless, the equivalent width of Lyman-α ($\sim$8 Å) is extremely low compared to those of other objects (20–80 Å; Francis et al. 1991).

2. OBSERVATIONS

2.1. *Optical Spectrophotometry*

We obtained optical spectrophotometry of the quasar during 1988 at the Multiple Mirror Telescope (MMT) using the Blue Channel and the Faint Object Grating Spectrograph (FOGS). Higher resolution data were obtained through a 1″ slit, and the flux level was normalized using lower resolution data through a 5″ slit. Mg II and C III emission lines are detected, together with stong Fe II emission. In an attempt to observe the region around rest frame Hβ, I. W. Browne, P. N. Wilkinson, and D. Henstock kindly obtained Faint Object Spectrograph (FOS) data on the 2.5 m Isaac Newton Telescope (INT) extending to 10000 Å. Unfortunately the spectral region in question sits on atmospheric absorption lines, but the presence of an Hβ line of normal strength can be ruled out. The normalization of all the spectra is in good agreement with CCD photometry obtained at the 0.6 m telescope of the F. L. Whipple Observatory in 1986. The combined optical spectrum is presented in Figure 1.

2.2. *Ultraviolet Observations*

The *IUE* spectra were retrieved from the National Space Science Data Center and analysed using the RDAF IDL package. The spectra were extracted and calibrated using the standard GEX Gaussian Extraction algorithm (Urry & Reichert 1988). *HST* data, taken as part of the Absorption Line Key Project (Bahcall et al. 1993), were retrieved from the Hubble Data Archive using Starview and analyzed with the STSDAS package. We adjusted the flux of the G160L observation, taken through the 0.″1 aperture, to match the data in the other gratings, taken through the 0.″25 × 2.″0 slit. We note that the G270H spectrum was not analyzed by Bahcall et al. because it covers wavelengths longward of Lyman-α. Weak O IV + Si IV and C IV lines are present in the *HST* spectrum (Fig. 2) and (less obviously) in the *IUE* data. The Lyman-α line is present but cut up with superposed absorption lines. Our value of 8 Å for the equivalent width of this line is approximate and based on an ad hoc linear continuum fit at 1300 Å and 1140 Å (Table 2). The *HST* data agree well in flux (to within 15%) with the 1989 and 1986 *IUE* data; the quasar's far-ultraviolet flux seems to have increased by 30% since the 1983 *IUE* observation. This degree of variability is normal in quasars (Kinney et al. 1991).

2.3. *Infrared Observations*

Infrared spectroscopy was obtained through a service observation carried out on UKIRT (the United Kingdom

[1] Center for Astrophysics, 60 Garden Street, Cambridge, MA 02138.
[2] Center for Space Research, 37-241, Massachusetts Institute of Technology, Cambridge, MA 02139.
[3] Edinburgh Institute for Astronomy, University of Edinburgh, Royal Observatory Edinburgh, Blackford Hill, Edinburgh EH9 3HJ, Scotland.
[4] Physics Department, PAS 81, University of Arizona, Tucson AZ 85721. Also Center for Space Research, MIT.

TABLE 1

LOG OF OBSERVATIONS

Telescope[a]	Instrument[a]	Date	Exposure Time (minutes)	Spectral Range	Observers	ID[b]
Einstein	IPC	1981 Jan 17	26	0.2–3.5 keV	CfA	I05381
IRAS	Survey	1983	...	12–100 μm	[Survey]	
VLA	...	1983 Nov	...	5 GHz	Kellerman et al.	
FLWO 0.6 m	CCD	1986 May 14	...	*BVRL*	Wilkes	
MMT	IR Photometry	1988 Apr 7	...	*JHKL*	Willner	
MMT	FOGS	1988 Apr 9	...	4500–8300 Å	Wilkes	
MMT	Blue Channel	1988 Jun 6	...	3200–6200 Å	Wilkes	
IUE	SWP	1983 Apr	356	1250–2000 Å	Snijders	SWP 19858
IUE	LWP	1986 Dec	400	2000–3100 Å	Bechtold	LWP 09733
IUE	LWP	1989 May 28	412	2000–3100 Å	O'Brien	LWP 15616
IUE	SWP	1989 May 28	395	1250–2000 Å	O'Brien	SWP 36351
ROSAT	PSPC	1992 Jan 19	54	0.15–2 keV	Canizares	RP 700359
HST	FOS/H19	1992 Mar 9	18	1590–2300 Å	Bahcall et al.	Y0RV0C03T, 04T
HST	FOS/H27	1992 Mar 9	18	2200–3250 Å	Bahcall et al.	Y0RV0C05T
HST	FOS/L15	1992 Mar 9	11	1170–2500 Å	Bahcall et al.	Y0RV0C06T
UKIRT	CGS4	1994 Jan 29	8	1.15–1.36 μm	UKIRT Service	
INT	FOS	1994 Feb 12	10	3650–10000 Å	Browne, Wilkinson, & Henstock	

[a] See main text for explanation of abbreviations.
[b] Sequence number or other designation in archive.

Infrared Telescope). The spectrum shown in Figure 3, which shows a strong Hα line at an observed wavelength of 1.28 μm, was obtained on 1994 January 29 with the cooled grating spectrometer CGS4, using the 150 mm camera and a 75 line mm^{-1} grating in second order, resulting in a spectral resolution corresponding to 780 km s^{-1} One resolution element is approximately equal to 1 detector pixel; however, the detector was stepped in increments of one-third of a pixel to improve sampling. The slit width used was 3″, roughly equal to 1 original detector pixel. Standard nodding, calibration, and atmospheric correction techniques were followed. Because of the large slit size, the wavelength calibration could potentially be offset if the object was not properly centered; any such error is certainly less than 400 km s^{-1}, and is probably much less.

JHKL photometry was obtained at the MMT in 1988 and shows the continuum inflection characteristic of a quasar. Examination of the *IRAS* sky images shows that PG 1407+265 is 3′ from the strong 60 μm source IRAS 14070+2636, which has been identified with the starburst galaxy Haro 40. Addscans of the *IRAS* survey data show no evidence for a 60 μm detection of the quasar, but we have reported a formal, marginal 25 μm detection (Elvis et al. 1994), although this should probably be treated with skepticism because it was not detected in any other *IRAS* band.

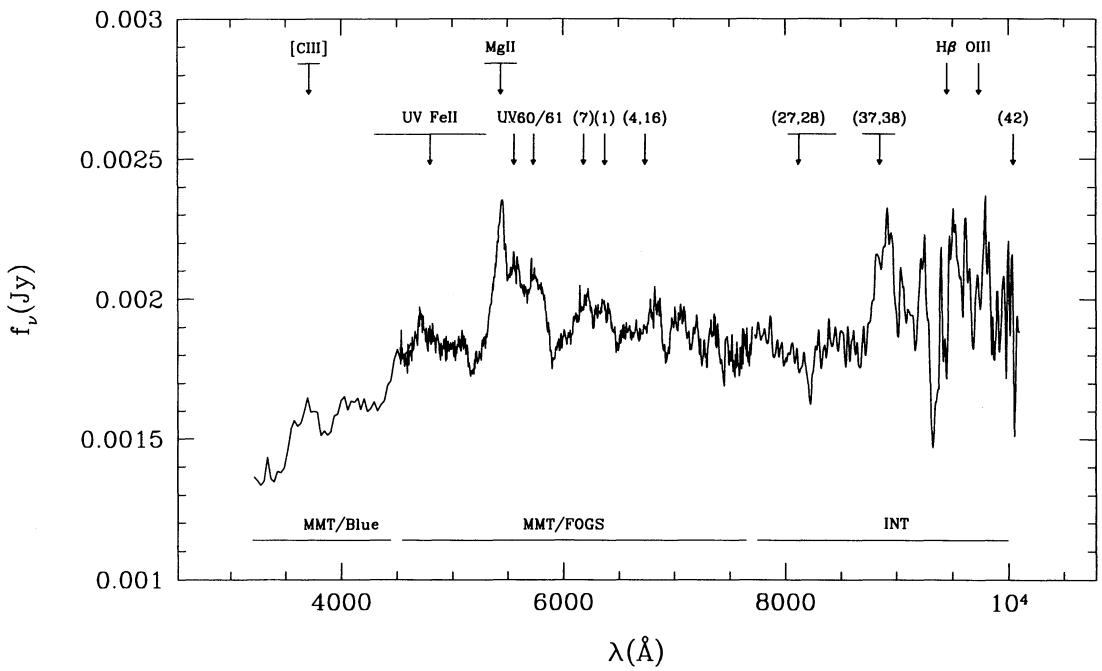

FIG. 1.—Optical spectrum of PG 1407+265. The plot shows the combined observations from the MMT Blue Channel and FOGS instruments and the INT. Expected ocations of emission lines and selected Fe II multiplets are indicated. The Blue Channel and INT data have been multiplied by a constant 12% factor to agree with the FOGS data.

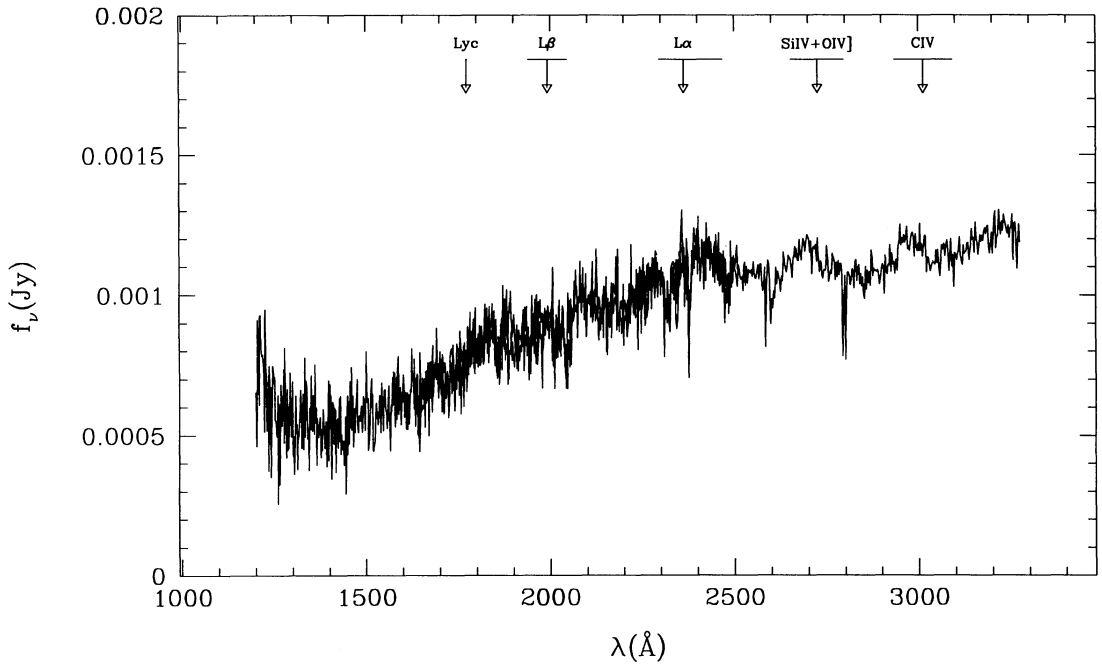

FIG. 2.—*HST* spectrum of PG 1407+265. The plot shows the combined observations from the G270H, G190H, and G160L gratings.

2.4. *X-Ray Observations*

PG 1407+265 was observed on 1992 January 19 with the *ROSAT* PSPC (Trümper 1983; Pfeffermann et al. 1987) for 3229 s. The source is well detected and is consistent with the point-spread function. We note that there is no evidence for any significant confusing source at the position of Haro 40 (Green et al. 1989) with a 3 σ upper limit of 1×10^{-13} ergs $cm^{-2}\ s^{-1}$ (0.4–2.4 keV).

We extracted counts from a 3′ circle around the position of PG 1407+265, together with background in an annulus from 3′.5 to 7′, using the IRAF/PROS package. The data were analyzed with the XSPEC spectral fitting package using the 1993 January (DRM 36) response matrix. We fitted a single power-law spectrum with Galactic absorption (Morrison & McCammon 1983). The data are consistent with this model, and the fitted absorption was consistent with the Galactic value of $1.38 \pm 0.10 \times 10^{20}$ cm^{-2} (Elvis, Lockman, & Wilkes 1989), so we repeated the fit with absorption fixed at this value. The best fit gave a power-law energy index of 1.61 ± 0.05 and a 1 keV flux of 1.0 ± 0.04 μJy, with a reduced χ^2 of 0.49 (Fig. 4). Consistent results were obtained using the SPECTRAL package in IRAF/PROS. We also set an upper limit to the amount of extra absorption (above Galactic) due to cold material at the redshift of the source of $N_H < 3.1 \times 10^{20}$ cm^{-2} (or 4.9×10^{19} cm^{-2} for extra absorbers at zero redshift); although there are no obvious edges in the spectrum, we cannot rule out the presence of an ionized absorber. Our derived power-law index is steeper than, but consistent with, the *Einstein* IPC result of $1.2^{+0.9}_{-0.2}$ (Wilkes & Elvis 1987); note that fits to PSPC data appear systematically steeper than the

TABLE 2

PG 1407+265: MEASURED REST FRAME EMISSION-LINE PROPERTIES

Line	Instrument	λ_{obs}	Redshift	EW (Å)	Luminosity (10^{44} ergs s^{-1})	Typical EW[a] (Å)
Lyα λ1215	*IUE*	...	...	<10	30–100	...
	HST	2370	0.95 ± 0.015	8 ± 3	10:	
O IV] + Si IV λ1400	*IUE*	2690	0.92 ± 0.01	9.1 ± 3	4.2	...
	HST	2675	0.912 ± 0.004	4.3 ± 2	2.2	
C IV λ1549	*IUE*	2960	0.91 ± 0.01	3.6 ± 2.5	1.5	20–50
	HST	2980	0.924 ± 0.004	4.6 ± 2	1.9	
C III] + Al III λλ1909, 1858	MMT/Blue	3700	0.94 ± 0.03	9.9	3.5	...
Mg II λ2798	MMT/Blue	5435	0.943 ± 0.003	23.5	4.6	50–80
	MMT/FOGS	5450	0.948 ± 0.0012	23.2	4.8	
	INT	5445	0.946 ± 0.002	11.6	2.2	
	SS91[b]	...	0.947	24.4	...	
Hβ λ4861	INT	...	...	<40	<2.2	
Hα λ6563	UKIRT	12850	0.958 ± 0.001	126.0	4.1	250–1200

[a] Typical equivalent widths for the samples of Francis 1993, Espey et al. 1989, Baker et al. 1994, and Baker 1994.
[b] Steidel & Sargent 1991.

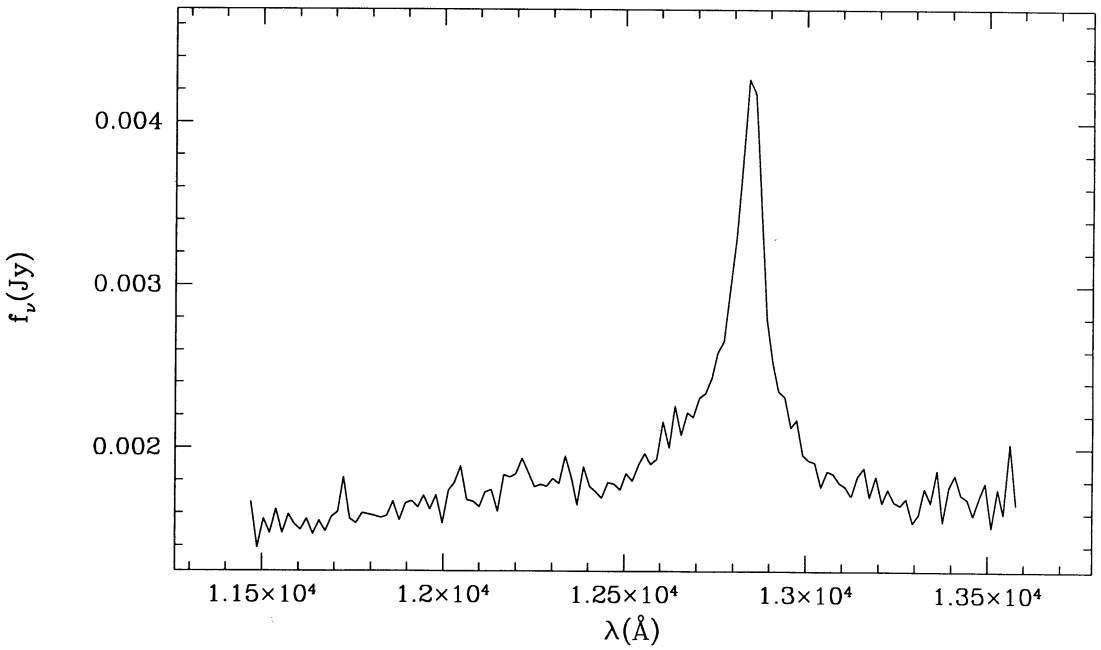

FIG. 3.—Infrared spectrum of PG 1407+265, obtained as a UKIRT service observation on 1994 January 29

IPC (Fiore et al. 1994). The normalization, however, is more than twice as high as the IPC value of 0.44 μJy, indicating significant X-ray variability over a timescale of a decade.

3. RESULTS

3.1. *The Redshift of PG 1407+265*

The initial published redshift estimate (Schmidt & Green 1983) was based on the single Mg II line. The failure to detect other lines in our intermediate signal-to-noise ratio spectrophotometry and in the *IUE* data raised the possibility that alternate (even nonquasar) identifications might be possible (Elvis et al. 1994).

Our observation of the strong Hα line in the near-infrared and our identification of the weak C IV and O IV] + Si IV lines in the *HST* data provide conclusive evidence that the redshift of the object is indeed near unity. The high-quality spectrum of Steidel & Sargent (1991) claimed to confirm the redshift as $z = 0.947$ and identified emission redward of Mg II as due to the λ2950 Fe II feature. However, the feature they claimed as C III] (observed wavelength 4019.4 Å; their Table 1) is incon-

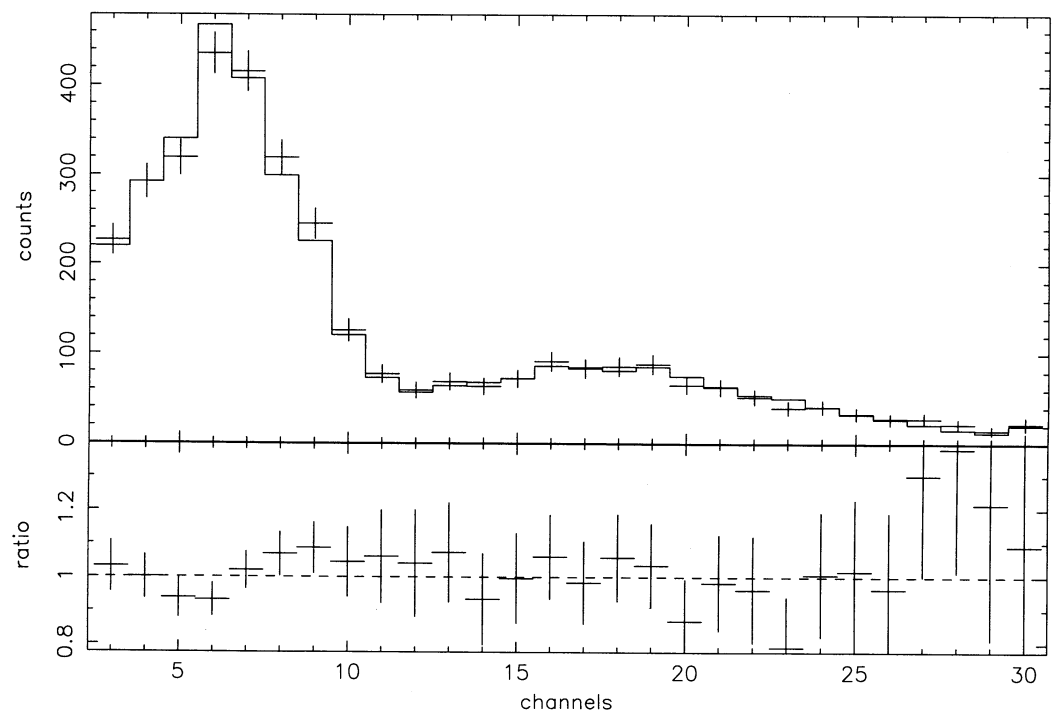

FIG. 4.—*ROSAT* PSPC pulse-height spectrum of PG 1407+265. The upper panel shows the extracted counts (*crosses*) and the fitted power-law model (*solid line*), while the lower panel shows the ratio of the counts to the model in each channel. The power-law model includes Galactic absorption of 1.38×10^{20} cm^{-2}.

sistent with this redshift; this feature corresponds to a weak unidentified line in the composite spectrum of Francis et al. (1991) and is not as strong in our MMT data. The true C III] + Al III feature is the weaker one visible in their spectrum at approximately the correct rest wavelength.

The wavelengths of the peaks of each emission line were measured and used to derive redshift estimates (Table 2). We quote nominal "1 σ" uncertainties which are one-third of our eyeball estimates of the maximum uncertainty in the peak location. As is typical for quasars, the redshifts of the low-ionization lines are larger than those of the high-ionization lines (Gaskell 1982; Wilkes 1984; Espey et al. 1989). However, the range in redshift for PG 1407+265 is an order of magnitude larger than typically seen: 10200 $\pm$ 1200 km s^{-1} between Hα and C IV compared with $\sim$1000 km s^{-1} in the earlier studies. The wavelength scales of the various instruments should be much better than this; the optical spectra were taken with the slit vertical to avoid refraction effects, although this is not an issue for the ultraviolet spectra, and refraction is small enough in the infrared to compensate for the larger slit width. Uncertainties in the velocity scale due to slit width and refraction effects should be less than 500 km s^{-1} in all cases.

Figure 5 shows the various emission lines on a common velocity scale with zero point set by Mg II. We see a significant trend of the velocity shift to increase with the ionization potential of the emission line (Fig. 6*a*). We note that a trend with rest wavelength is almost equivalent (Fig. 6*b*). We suggest that $z = 0.94 \pm 0.02$ is a reasonable statement of our knowledge of the quasar's redshift. Note in Figure 5 that there is a narrow absorption feature in Lyman-α coincident with the velocity of the Hα emission line, implying some overlaid neutral hydrogen component.

We also measured approximate line widths and fluxes. C IV λ1549 and the broad component of Hα both have full width at half-maximum (FWHM) around 7000 km s^{-1}. Mg II has a similar component but with a broad red-wing "shelf" of blended Fe II UV multiplets leading to a formal FWHM of around 12,000 km s^{-1}. C III] λ1909 appears to be equal in flux with Al III λ1858, although our spectrum has a low-signal-to-noise ratio in this region.

3.2. *Line Properties*

The emission lines in PG 1407+265 appear unusually weak when viewed by eye. How extreme are these equivalent widths? Table 2 gives the details of our measured values, including estimates of the integrated rest frame luminosity in each line. Typical emission-line properties of quasars are given in Table 12.4 of Osterbrock (1989) and for a subset of lines in Francis et al. (1991). While the Osterbrock data are not based on any specific sample, the latter paper gives average properties of the well-defined Large Bright Quasar Survey. Further, Francis (1993) gives histograms of equivalent width for the bright ultraviolet lines which may be used to measure how unusual PG 1407+265 actually is, although their spectral signal-to-noise ratio is too low to give reliable measurements for individual objects at the low equivalent widths we are probing.

The O IV] equivalent width, W(O IV]), is relatively normal in PG 1407+265, only a factor of 2 low. However, W(Lyα) is in the bottom 3% of the Francis et al. distribution (typical values 30–100 Å), as is the C IV strength (typically 20–50 Å), while W(Mg II) is in the lowest 4% of its corresponding distribution (typical values 50–80 Å). Quasar Hα equivalent widths are still hard to find, with results from several groups (Baker et al. 1994; Baker 1994) indicating that typical values are in the range 250–1200 Å, consistent with the early data of Baldwin (1975). However, we note that three objects in the sample of Espey et al. (1989) have values between 140 and 150 Å, comparable to our value of W(Hα) = 126 Å. We may summarize by saying that most of the line *ratios* in PG 1407+265 are not exceptional within the large uncertainties, but the equivalent widths for the principal lines are anomalously weak by factors of 3–10. In contrast, the Fe II multiplets (both optical and UV) appear to be unusually strong.

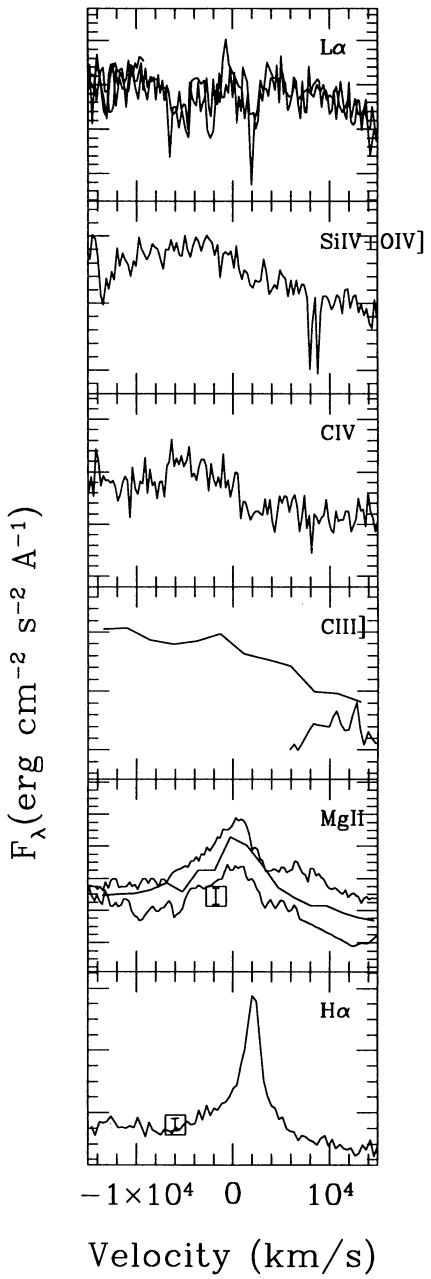

FIG. 5.—PG 1407+265 emission lines plotted on a common velocity scale. The zero point corresponds to the Mg II redshift. There are several Mg II spectra superposed (MMT Blue, FOGS, and the INT data) and two *HST* exposures superposed for Lyman-α. Squares in Mg II and Hα boxes correspond to broadband photometry measurements.

3.3. *Continuum Properties*

In contrast to the lines, the continuum properties of PG 1407+265 are remarkably normal. We present the dered-

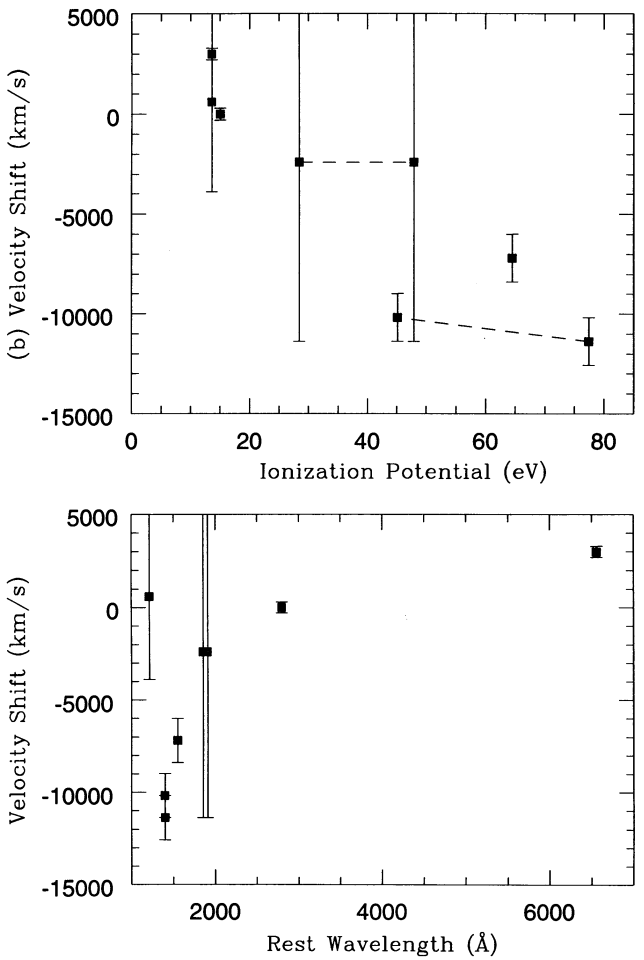

FIG. 6.—PG 1407+265 estimated line velocities vs. (*top*) ionization potential and (*bottom*) rest wavelength. The velocity zero point corresponds to the Mg II redshift. The dashed lines in the top panel connect the components of line blends, since those points are not independent.

dened, rest frame infrared–to–X-ray energy distribution in Figure 7 and a close-up of the optical-to-ultraviolet region in Figure 8. The radio-loudness (log of 5 GHz to optical *B*-band flux) is 0.28, within the normal range (Kellerman et al. 1989; Elvis et al. 1994) for radio-quiet objects. The 8 mJy, 5 GHz radio source is unresolved, although there is a probably unrelated weak source 1′ away (Kellerman et al. 1994). The blue bump strength is log [L(1000–2000 Å)/L(0.8–1.6 μm)] = 0.69, indistinguishable from the median value of 0.66 for the UVSX sample of Elvis et al. (1994), of which it is a member (see Fig. 7, which shows the 68th percentile ranges of that sample). The absolute continuum level in our 1988 MMT observations agrees with the Palomar observations of Neugebauer et al. (1987) made in 1980 to within 15%, as seen in a number of other objects in the survey of Elvis et al. *IUE* and *HST* observations are consistent with mild variations typical of quasars (Kinney et al. 1991). The presence of an inflection in the energy distribution between *H* and *K*, the *Einstein* IPC X-ray spectral index of 1.2 and *ROSAT* index of 1.6, and the low radio flux (Kellerman et al. 1989) are all consistent with a normal, nonvariable, radio-quiet quasar. The factor of 2 variability in the X-ray flux is somewhat unusual but not unprecendented for high-luminosity quasars (Zamorani et al. 1984). There is therefore no evidence for any underlying variable, beamed, blazar-like continuum component which may reduce the strength of the emission lines in some flat-spectrum radio quasars.

4. DISCUSSION

The emission-line spectrum of PG 1407+265 is unlike that of any other radio-quiet quasar we have seen, e.g., of ~100 in Elvis et al. (1994), Kinney et al. (1991), and Boroson & Green (1993). In Figure 8, we contrast the 1000–8000 Å rest frame spectrum of PG 1407+265 with comparable data for the ordinary, low-redshift quasar PG 1211+143. The difference in the amount of energy in the ultraviolet lines is dramatic. We now consider several possible explanations for the weak lines and differential redshifts of PG 1407+265.

1. *Not a quasar.*—Prior to the detection of Hα, we had speculated that the object might not be a quasar at all. That line and the overall multiwavelength continuum properties rule out that possibility.

2. *A beamed continuum.*—The lines are washed out by a beamed, nonthermal component (a jet along the line of sight). This solution, which would be unprecedented in a radio-quiet object, is ruled out by the lack of continuum variability and the normal shape of the energy distribution.

3. *Low BELR covering factor.*—The broad emission line region (BELR) has a lower covering factor, intercepting less of the continuum radiation. This simple explanation accounts for the low equivalent widths of the emission lines which originally drew our attention to the object but does not address the bizarre C IV and O IV line shifts.

4. *Abnormal photoionizing continuum.*—The weakness of the lines is intrinsic and due to an abnormal photoionizing continuum as seen by the line-emitting region. Although the continuum we see is normal, we may be looking at a special angle. If there is obscuration between the central source and most of the BELR (except along our line of sight), this might occur, although we have not tried to reproduce the observed spectrum with a photoionization code. Since objects like PG 1407+265 are clearly rare (a few percent at most), explanations involving special geometry are reasonable.

5. *Time lags.*—The UV continuum has recently brightened, and the lines have not yet caught up. The lack of optical and UV variability on a 10 yr timescale casts doubt on this, although the factor of 2 increase in the X-ray since 1981 is worth noting. This explanation would imply an effective BELR radius large compared with 10 lt-yr, while scaling with the expected $L^{1/2}$ dependence from NGC 5548 (Clavel et al. 1991) would predict a much smaller BELR radius, ~1 lt-yr.

6. *Abnormal BELR physical properties.*—The weakness of the lines is intrinsic and due to abnormal cloud properties in the broad emission line region. Before the detection of Hα, the possibility of "hydrogen-depleted" clouds was tenable (if physically unlikely). The presence of Hα requires some other peculiarity: the size or density of the clouds may be unusual, or the distance of the BELR gas from the central object may be abnormal, leading to an unusual ionization parameter.

7. Fe II–*dominated continuum.*—The emission lines have a normal equivalent width with respect to the true continuum but are masked by strong Fe II emission as in IRAS 07598+6508 (Lawrence et al. 1988). This might work for some of the optical lines but cannot contribute to the weakness of C IV and Lyman-α.

8. *Dust absorption.*—The weakness of the short-wavelength lines is due to patchy reddening between us and the quasar

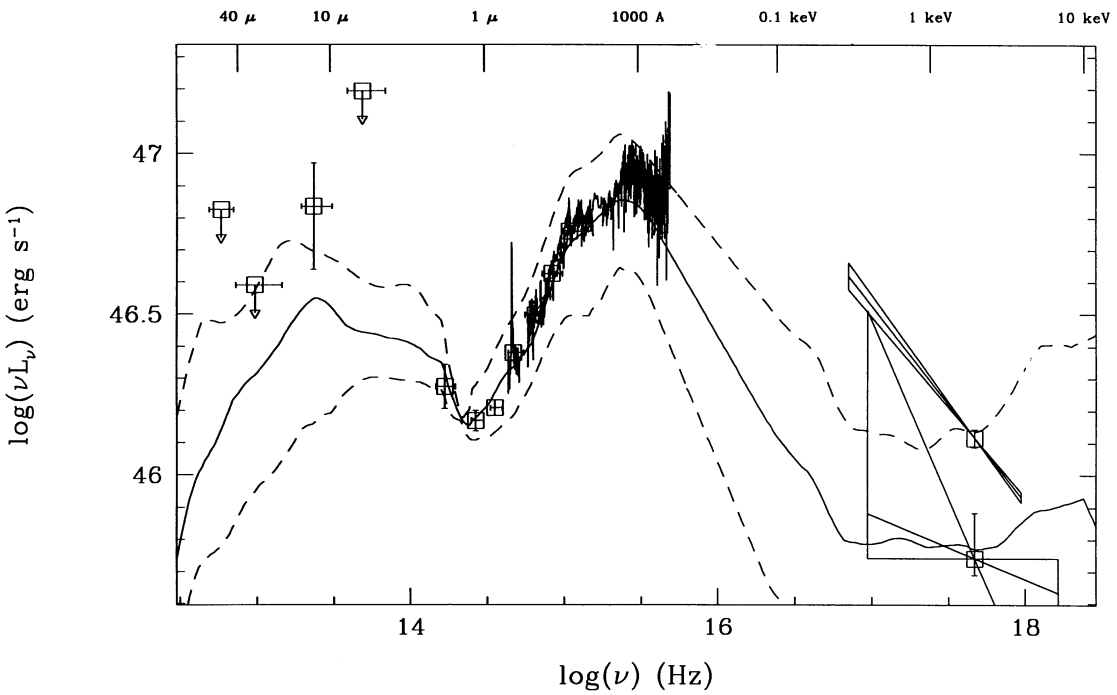

FIG. 7.—Rest frame spectral energy distribution for the quasar PG 1407+265. Observations have been corrected for Galactic foreground reddening with $E(B-V) = 0.03$. The X-ray data points show power-law fits to the *Einstein* and *ROSAT* data with 90% slope errors indicated. Solid and dashed lines indicate median quasar spectral energy distribution and 68th percentile deviations from Elvis et al. (1994).

nucleus. This is unlikely since the continuum source shows no evidence of reddening: the ultraviolet continuum is strong, and the soft X-rays show no significant absorption in excess of Galactic. The absence of a definite *IRAS* detection implies (Fig. 6) that the object is not exceptionally far-infrared bright, unlike some of the Fe II emitters studied by Lawrence et al. (1988), and so most of the continuum cannot be reprocessed by dust. Any explanation based on reddening must therefore explain how the lines but not the continuum are affected.

9. *Line absorption.*—PG 1407+265 is a weak BAL quasar in which the absorption lines are eating away at the emission. Note that the Lyman-α region (Fig. 3) appears to contain narrow absorption lines, although there is no evidence for any Lyman-continuum break, so $N_H \leq 10^{17}$ cm^{-2}. Patchy absorption leaves the continuum source unaffected, while most of the BELR emission is soaked up in a broad absorption line (BAL) region lying between us and the high-ionization region of the BELR generating C IV and O IV]. This explanation can address the observed redshift differences. The velocity of the BAL clouds is such that the red wing and center of the BELR lines are preferentially absorbed. The remaining blue wing gives an artificially low redshift. The low-ionization emission lines, which are generated farther from the nucleus, suffer less or no red BAL absorption and give the true emission redshift, which is nearer to $z = 0.95$. The problem with this picture, as with dust absorption, is the low probability that the bulk of the emission lines would be absorbed without affecting the continuum source.

10. *Gravitational amplification.*—The equivalent widths are low because the continuum source is magnified by a stellar mass microlens along the line of sight. Dalcanton et al. (1994) set probabilities on the cosmological density of lensing objects based on the absence of weak equivalent width objects in some quasar samples; to cast their argument slightly differently, if microlensing has any significant effect on the quasar population, we should expect it to show up in a few high-luminosity, bright objects with weak equivalent widths. PG 1407+265 is a factor of 25 more luminous than the median PG quasar from Schmidt & Green (1983) and only a magnitude less luminous that the multiple-image lens PG 1115+080. This interpretation would predict that the continuum is likely to fade on a timescale of decades (for a 1 $M_\odot$ lens; Dalcanton et al. 1994). However, the apparent strength of the Fe II emission, which would be unlensed, counts against this explanation. A quantitative measurement of the strength of Fe II (opt), not really possible with our current data because of the low signal-to-noise ratio near Hβ, would be important in evaluating the possibility of lensing. Deep CCD imaging could reveal the presence of any lensing galaxy at $z \sim 0.5$.

5. CONCLUSION

We have presented observations of an unusual quasar, PG 1407+265. The quasar has a normal nonvariable, radio-quiet continuum energy distribution, but the high-ionization emission lines are extremely weak and strongly blueshifted with respect to the low-ionization lines. We have discussed 10 possible explanations for the unusual spectrum, none of which is immediately convincing. Higher signal-to-noise ratio observations of the lines and detailed modeling will be required to resolve the mystery of PG 1407+265.

We acknowledge support from STScI grant AR-3686.01-91A, NASA grants NAGW5-2201 (LTSA), NAS 5-30934 (RSDC), and use of IPAC's National Extragalactic Database (NED), the Goddard Space Flight Center's *IUE* data analysis facility and HEASARC X-ray archive, and of the Hubble Data Archive.

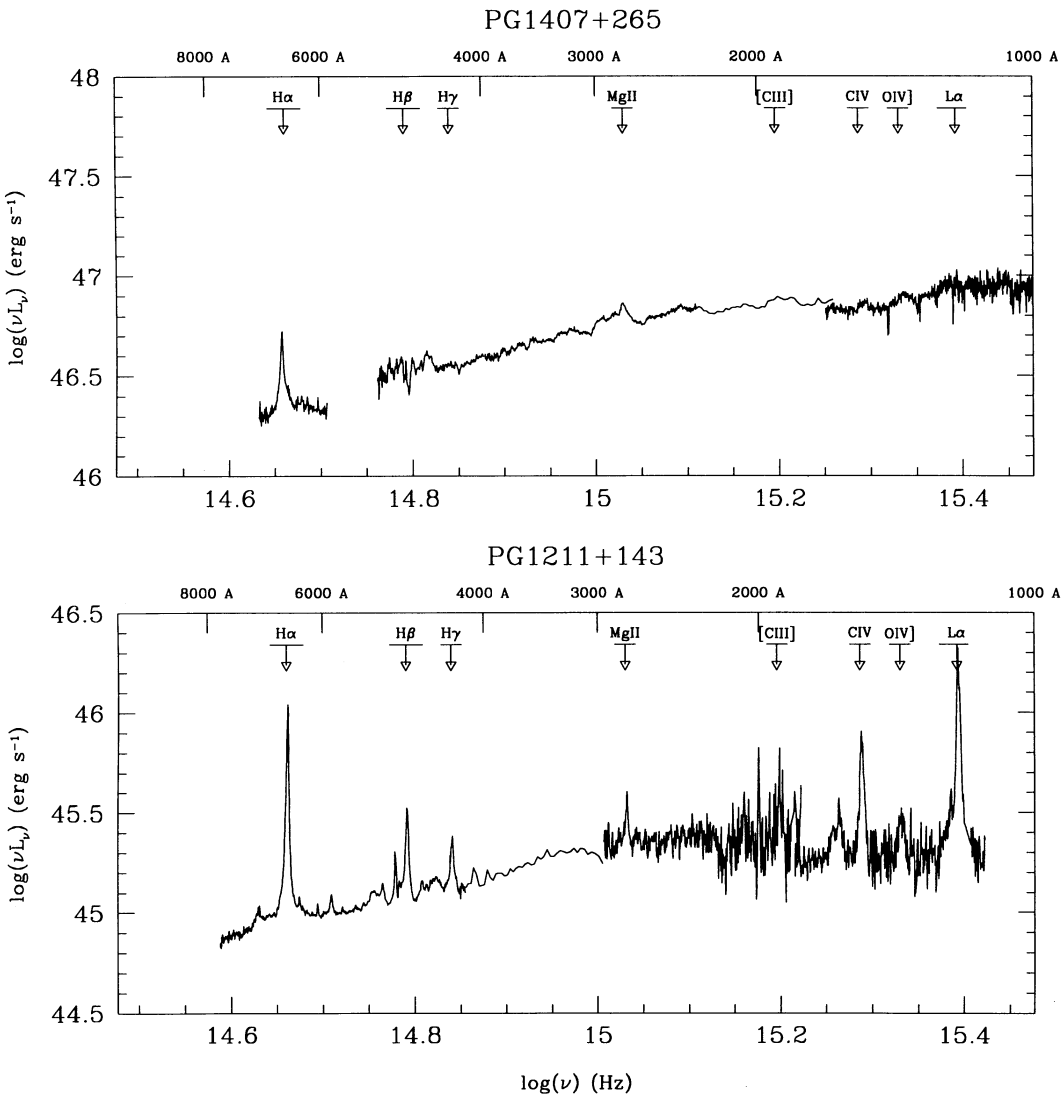

FIG. 8.—Optical and ultravoiolet rest frame energy distribution for PG 1407+265 compared with that of PG 1211+143 (data from Elvis et al. 1994). The plots cover the same range in logarithmic flux, so lines of identical equivalent width will appear the same. Line identifications are indicated.

REFERENCES

Bahcall, J., et al. 1993, ApJS, 87, 1
Baker, A. C., et al. 1994, MNRAS, 270, 575
Baker, J. C. 1994, Ph.D. thesis, Univ. of Sydney
Baldwin, J. 1975, ApJ, 201, 26
Berriman, G., Schmidt, G. D., West, S. C., & Stockman, H. S. 1990, ApJS, 74, 869
Boroson, T., & Green, R. F. 1993, ApJS, 80, 109
Clavel, J., et al. 1991, ApJ, 366, 64
Dalcanton, J. J., Canizares, C. R., Granados, A., Steidel, C. C., & Stocke, J. T. 1994, ApJ, 424, 550
Elvis, M., et al. 1994, ApJS, 95, 1
Elvis, M., Lockman, F. J., & Wilkes, B. J. 1989, AJ, 97, 777
Espey, B., et al. 1989, ApJ, 342, 666
Fiore, F., et al. 1994, ApJ, 431, 575
Francis, P. J. 1993, ApJ, 405, 119
Francis, P. J., et al. 1991, ApJ, 373, 465
Gaskell, C. M. 1982, ApJ, 263, 79
Green, P. J., Ward, M. J., Anderson, S. F., Margon, B., De Grijp, M., & Miley, G. K. 1989, ApJ, 339, 93
Kellerman, K. I., et al. 1989, AJ, 98, 1195
Kellerman, K. I., et al. 1994, AJ, 108, 1163
Kinney, A., et al. 1991, ApJS, 75, 645
Lawrence, A., et al. 1988, MNRAS, 235, 261
Morrison, R., & McCammon, D. A. 1983, ApJ, 270, 119
Neugebauer, G., et al. 1987, ApJS, 63, 615
Osterbrock, D. 1989, Astrophysics of Gaseous Nebulae and Active Galactic Nuclei (Mill Valley: Univ. Sci. Books)
Pfefferman, E., et al. 1987, Proc. SPIE, 733, 519
Schmidt, M., & Green, R. F. 1983, ApJ, 269, 352
Steidel, C. C., & Sargent, W. L. W. 1991, ApJ, 382, 433
Trümper, W. 1993, Adv. Space Res., 2(4), 241
Urry, C. M., & Reichert, G. 1988, NASA *IUE* Newsletter, 34, 95
Wilkes, B. J. 1984, MNRAS, 207, 73
Wilkes, B. J., & Elvis, M. 1987, ApJ, 323, 343
Zamorani, G., et al. 1984, ApJ, 278, 28

Note added in proof.—M. Corbin (ApJ, 357, 346 [1990]) points out that PG 1407+265 lies on an extrapolation of the velocity shift–C IV equivalent width correlation discovered by him.